Automated Computation of the Vascular Input Function for Dynamic Contrast-Enhanced MRI of the Brain

S. N. Gupta[1], J. A. Butman[2]

[1]Applied Science Lab, GE Healthcare, Hanover, MD, United States, [2]Diagnostic Radiology Dept., Clinical Center, NIH, Bethesda, MD, United States

Introduction

Dynamic contrast-enhanced MRI (DCEMRI) is being increasingly used to characterize and quantify contrast medium behavior in tumors and tissues. Pharmacokinetic modeling of dynamic data obtained successively during treatment has shown that the changes in the kinetic parameters correlate with histopathological outcomes thereby demonstrating the promise of this technique in staging tumors and in monitoring response to therapy [1,2]. The 2-compartment General Kinetic Model (GKM) describes the kinetics of contrast exchange between the plasma and the extracellular extravascular space based on 3 parameters (K^{trans}, k_{ep}, and f_{PV}). Although some approaches assume a particular form of a vascular input function, solving the GKM using a measured vascular input function (VIF) makes the model flexible in accounting for different infusion protocols and patient specific differences. Manual identification of an accurate and representative VIF is time-consuming and difficult, and adds to variability making it less reproducible and more prone to errors due to the incorrect placement of the region of interest (ROI) and flow and other artifacts.

In this work, a fast, fully automatic method for estimating the VIF from 3D brain DCEMRI data is developed, based on a method originally used to obtain input function for dynamic susceptibility contrast MRI [3]. This method consists of first computing a mask from the dynamic data to emphasize the vasculature, and then selecting pixels from this mask which exhibit enhancement characteristics of vessels with a high degree of confidence. Results comparing the automatic VIF with expert-drawn manual VIF on 15 clinical cases are presented.

Methods

Acquisition: 15 patients with brain tumors were scanned on a 1.5T Signa CV/i MRI scanner (GE Healthcare, Waukesha, WI) under IRB approved protocols, using a 3D SPGR sequence (TR/TE 7.2/3.1ms, FA 30°, BW ±31 kHz, FOV 22 cm, matrix 256 x 192 x 16, slab 8 cm). In each study 30 volumes were obtained in 10 mins (20 sec/volume). 0.1 mmol/kg Gd-DTPA was injected i.v at 0.3 cc/sec for 100 seconds (Figure 1a).

Manual VIF Selection: DICOM data was processed using a pharmacokinetic analysis package (Cinetool, GE Healthcare) custom built in IDL. Following inspection of the time series data, a small ROI was placed within a large venous sinus to generate the manual VIF. An inferior slice location was selected to eliminate effects of inflow. Because the temporal scale was 20 seconds per volume and the capillary transit time is on the order of 4 seconds, we assume that venous and arterial concentrations are well mixed and effectively identical, hence we use the term "vascular input function" rather than "arterial input function." ROIs were selected in veins as they are larger than arteries and afford a greater opportunity to identify pure blood voxels with no volume averaging.

Automatic VIF Estimation: First, an inferior slice location was selected. Second, bolus arrival time and time to peak were calculated automatically based on a single averaged signal intensity vs. time curve for the entire slice. Third, a baseline standard deviation (SD) map was created (Figure 1b) using the standard deviation over time from time 0 to the arrival time for each pixel. Similarly, a contrast SD map (Figure 1c) was created using the standard deviation from time 0 to the peak time. Subtracting these two yields a mask image (Figure 1d) which selectively emphasizes rapidly enhancing tissues such as the vasculature and eliminates variation due to noise. Finally, by adjusting a user-controllable threshold (% of mask maximum), candidate vascular pixels could be reliably selected (These pixels are shown in red in Figure 1d). In all our studies, a threshold of 0.6 reliably selected 50-100 pixels all of which were anatomically identified to be within the vasculature. The signal from these pixels was averaged to estimate the VIF.

Modeling: Gd concentration vs. time curves were computed by performing T_1 correction (assuming blood T_1 = 1.32 s), calculating change in relaxivity from the SPGR equation, and converting to concentration (assuming Gd-DTPA relaxivity = 4.9 s^{-1} mM^{-1}). Parametric maps were computed by iteratively adjusting K^{trans}, k_{ep}, and f_{PV} so that the convolution of the VIF with the transfer function fits the data at each voxel location.

Results

The VIF curves obtained by the two methods were highly correlated as shown by the point-wise scatter plot in Figure 2 (R^2=0.97). The root mean square error between the two in all 15 subjects was 15.2 ± 5.3 %. The VIFs generated by the automatic method were systematically higher than those obtained by the manual ROI, peak Gd concentration was 18.4% higher and the area under the curve (AUC) was 12.6% higher. Figure 3 shows an example of the automatic VIF and manual VIF on the same subject. It also shows the error (difference) between the two methods on all 15 subjects plotted on the same scale. The time to peak matched perfectly between the two methods in 14 of the 15 cases and was off by 1 time point in 1 case. Sample K^{trans} parametric maps from one dataset by using the manual VIF and the automatic VIF are shown in Figures. 4a and b respectively. No visual differences were found comparing the parametric maps in all cases.

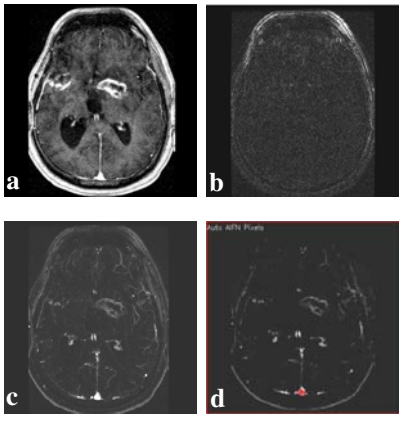

Figure 1

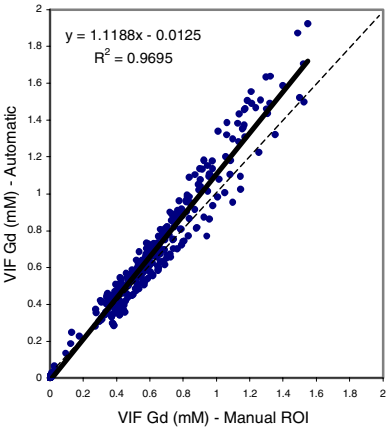

Figure 2

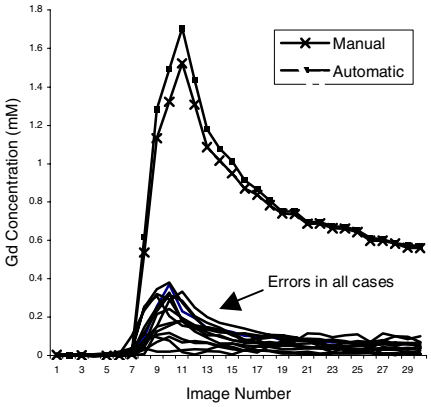

Figure 3

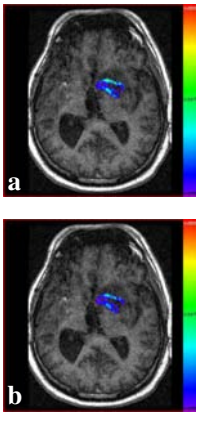

Figure 4

Conclusion

We have presented a fast, fully automatic method for estimating the VIF from DCEMRI data of the brain, and shown that this method obtains a VIF in good agreement with those derived by a manual hand-drawn ROI. Manual ROI placement may, in fact, be more prone to volume averaging and systematically underestimate the true VIF. Use of an automated method should lead to more efficient and less user-dependent and therefore more reproducible analysis of DCEMRI data. Extending this method to other DCEMRI protocols such as breast, prostate etc. is possible and is being explored further.

References

[1] Padhani, *JMRI* 16:407-422; 2002.
[2] Knopp et al., *Topics in MRI* 12(4):301-308; 2001.
[3] Butman et al., *Proc.ISMRM* 2005: p1126.